

Observation of the Anomalous Shape of $X(1840)$ in $J/\psi \rightarrow \gamma 3(\pi^+\pi^-)$ Indicating a Second Resonance Near $p\bar{p}$ Threshold

M. Ablikim *et al.**
(BESIII Collaboration)

 (Received 2 November 2023; revised 16 January 2024; accepted 23 February 2024; published 9 April 2024)

Using a sample of $(10087 \pm 44) \times 10^6 J/\psi$ events, which is about 45 times larger than that was previously analyzed, a further investigation on the $J/\psi \rightarrow \gamma 3(\pi^+\pi^-)$ decay is performed. A significant distortion at 1.84 GeV/ c^2 in the line shape of the $3(\pi^+\pi^-)$ invariant mass spectrum is observed for the first time, which could be resolved by two overlapping resonant structures, $X(1840)$ and $X(1880)$. The new state $X(1880)$ is observed with a statistical significance larger than 10σ . The mass and width of $X(1880)$ are determined to be $1882.1 \pm 1.7 \pm 0.7$ MeV/ c^2 and $30.7 \pm 5.5 \pm 2.4$ MeV, respectively, which indicates the existence of a $p\bar{p}$ bound state.

DOI: [10.1103/PhysRevLett.132.151901](https://doi.org/10.1103/PhysRevLett.132.151901)

A distinct resonance, $X(1835)$ [1], in the $\pi^+\pi^-\eta'$ invariant mass spectrum and a dramatic $p\bar{p}$ mass threshold enhancement [2] in $J/\psi \rightarrow \gamma p\bar{p}$ were first observed by BESII, which stimulated both theoretical and experimental interests in their nature. Some theoretical models are proposed to interpret their internal structures, e.g., a $p\bar{p}$ bound state [3–6], a pseudoscalar glueball [7–9], or a radial excitation of the η' meson [10]. Subsequently, these resonances were confirmed by BESIII [11,12] and CLEO [13] experiments and found to have the same J^{PC} of 0^{-+} [14,15]. Meanwhile, a prominent structure $X(1840)$ was observed in the $3(\pi^+\pi^-)$ invariant mass [$M(6\pi)$] spectrum in $J/\psi \rightarrow \gamma 3(\pi^+\pi^-)$ with a mass of $1842.2 \pm 4.2_{-2.6}^{+7.1}$ MeV/ c^2 and a width of $83 \pm 14 \pm 11$ MeV [16]. It was interpreted as a new decay mode of $X(1835)$, although its width is substantially narrower than that of $X(1835)$ [12]. Of interest is that an updated analysis of $J/\psi \rightarrow \gamma \pi^+\pi^-\eta'$ observed a significant abrupt change in slope of the $X(1835) \rightarrow \pi^+\pi^-\eta'$ line shape at the $p\bar{p}$ mass threshold, which could be originated from the opening of an additional $p\bar{p}$ decay channel (threshold effect) or the interference between two different resonance contributions [17]. To understand whether a similar phenomenon to that of $J/\psi \rightarrow \gamma \pi^+\pi^-\eta'$ exists around the $p\bar{p}$ mass threshold in the $M(6\pi)$ spectrum, it is worth a more detailed investigation on the $X(1840)$ line shape in $J/\psi \rightarrow \gamma 3(\pi^+\pi^-)$ with higher precision. In this Letter we report an anomalous line shape of $X(1840)$ in the $M(6\pi)$ spectrum in

$J/\psi \rightarrow \gamma 3(\pi^+\pi^-)$ with a sample of $(10087 \pm 44) \times 10^6 J/\psi$ events [18] collected with the BESIII detector. The size of the sample is about 45 times greater than that used in Ref. [16].

The BESIII detector records symmetric e^+e^- collisions provided by the BEPCII storage ring [19] in the center-of-mass energy range from 2.0 to 4.95 GeV, which is described in detail in [20–23]. Simulated data samples produced with a GEANT4-based [24] Monte Carlo (MC) package, which includes the geometric description of the BESIII detector [25] and the detector response, are used to determine detection efficiencies and to estimate backgrounds. The simulation models the beam energy spread and initial state radiation in the e^+e^- annihilation with the generator KKMC [26]. All particle decays are modeled with EVTGEN [27,28] using branching fractions either taken from the Particle Data Group [29], when available, or otherwise estimated with LUNDCHARM [30,31]. Final state radiation from charged final state particles is incorporated using the PHOTOS package [32].

Charged tracks detected in the main drift chamber (MDC) are required to be within a polar angle (θ) range of $|\cos\theta| < 0.93$, where θ is defined with respect to the z axis, the symmetry axis of the MDC. The distance of closest approach to the interaction point must be less than 10 cm along the z axis, and less than 1 cm in the transverse plane. Photon candidates are reconstructed using clusters of energy deposited in the electromagnetic calorimeter (EMC), where a minimum energy of 25 MeV for the barrel region ($|\cos\theta| < 0.8$) and 50 MeV for the end cap region ($0.86 < |\cos\theta| < 0.92$) is required. To suppress electronic noise and showers unrelated to the event, the difference between the EMC time and the event start time is required to be within [0, 700] ns.

*Full author list given at the end of the Letter.

Published by the American Physical Society under the terms of the [Creative Commons Attribution 4.0 International license](https://creativecommons.org/licenses/by/4.0/). Further distribution of this work must maintain attribution to the author(s) and the published article's title, journal citation, and DOI. Funded by SCOAP³.

Candidates for the signal are required to have six charged tracks with zero net charge and at least one photon. All the charged tracks are assumed to be pions. A four-momentum-constraint (4C) kinematic fit is performed under the hypothesis of $J/\psi \rightarrow \gamma 3(\pi^+\pi^-)$, and the χ^2_{4C} of this kinematic fit is required to be less than 30. For events with more than one photon candidate, the $\gamma 3(\pi^+\pi^-)$ combination with the minimum χ^2_{4C} is retained. To suppress the backgrounds with a final state of $\gamma\gamma 3(\pi^+\pi^-)$, the χ^2_{4C} is required to be less than that for the kinematically similar $\gamma\gamma 3(\pi^+\pi^-)$ hypothesis. Furthermore, for the events containing at least two photons, the $\gamma\gamma$ invariant mass is required to be outside the π^0 mass window of $|M_{\gamma\gamma} - m_{\pi^0}| < 0.01 \text{ GeV}/c^2$ to veto the backgrounds with π^0 in their final states.

The $J/\psi \rightarrow \gamma K_S^0 K_S^0 \pi^+ \pi^-$ process with a subsequent decay of K_S^0 to $\pi^+ \pi^-$ has the same final state as the signal decay. To suppress this background, the K_S^0 candidates are reconstructed from secondary vertex fit (SVF) to all $\pi^+ \pi^-$ pairs. The K_S^0 candidates are tagged by passing the SVF successfully and requiring the $\pi^+ \pi^-$ invariant mass in a range of $|M_{\pi^+\pi^-} - m_{K_S^0}| < 0.005 \text{ GeV}/c^2$, where $m_{K_S^0}$ is the K_S^0 known mass. Given the existence of misreconstructed K_S^0 for the signal, events with the number of K_S^0 candidates less than 2 are retained for further analysis.

After applying the above requirements, the $M(6\pi)$ spectrum is shown in Fig. 1, where, in addition to the well established η_c peak and the peak around $3.07 \text{ GeV}/c^2$ from $J/\psi \rightarrow 3(\pi^+\pi^-)$ background channel, a distinct structure around $1.84 \text{ GeV}/c^2$ is apparent, and an anomalous line shape near the $p\bar{p}$ mass threshold is clearly observed, as shown in the inset plot.

With exactly the same processes of simulated inclusive J/ψ events as for the data, no peaking background contribution around $1.84 \text{ GeV}/c^2$ is found. The remaining background is mainly from $J/\psi \rightarrow \pi^0 3(\pi^+\pi^-)$, for which,

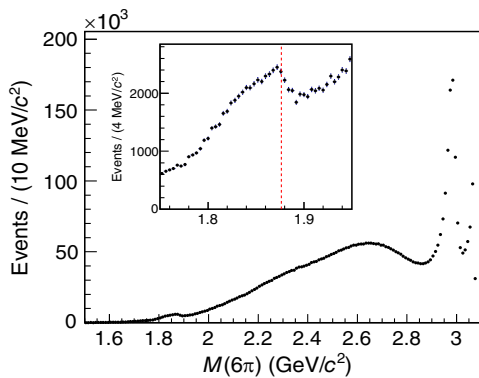


FIG. 1. $M(6\pi)$ distribution from $J/\psi \rightarrow \gamma 3(\pi^+\pi^-)$ events. The dots with error bars are data. The inset shows the data between 1.75 and $1.95 \text{ GeV}/c^2$ and the vertical dotted line represents the $p\bar{p}$ mass threshold.

we use a one-dimensional data-driven method to determine its contribution. We select the $J/\psi \rightarrow \pi^0 3(\pi^+\pi^-)$ events from data first and then implement the signal selection criteria on these events. The $M(6\pi)$ spectrum extracted based on these surviving events is further reweighted by the ratio of MC-determined efficiencies for $J/\psi \rightarrow \gamma 3(\pi^+\pi^-)$ to $J/\psi \rightarrow \pi^0 3(\pi^+\pi^-)$ events. To ensure that the anomalous line shape in data is not caused by the distortion of the detection efficiency due to event selection bias, we studied the phase space MC events of $J/\psi \rightarrow \gamma 3(\pi^+\pi^-)$. As a result, neither the $1.84 \text{ GeV}/c^2$ peaking structure nor the abrupt change in the line shape near the $p\bar{p}$ mass threshold is caused by the background processes or the distortion of the event selection efficiency.

We perform an unbinned maximum likelihood fit to the $M(6\pi)$ spectrum between 1.55 and $2.07 \text{ GeV}/c^2$ with the $X(1840)$ peak represented by the efficiency corrected Breit-Wigner (BW) function convolved with a Gaussian function to account for the mass resolution, which is determined to be $4 \text{ MeV}/c^2$ from the MC simulation. The dominant background to the $X(1840)$ peak is from the nonresonant contribution of $J/\psi \rightarrow \gamma 3(\pi^+\pi^-)$, whose shape is obtained through MC simulation and the fraction is free in the fit. The $J/\psi \rightarrow 3(\pi^+\pi^-)\pi^0$ background contributions are estimated with the data-driven approach as described above. The remaining background is described by a free second-order polynomial function. Without explicit mention, all components are treated as incoherent contributions. The fit quality is significantly poor, as shown in Fig. 2. The goodness of fit is studied using a χ^2 test and the χ^2 value per number of degrees of freedom (N_{dof}) is found to be $\chi^2/N_{\text{dof}} = 399.0/45$. This implies that a simple resonant structure fails to describe the $M(6\pi)$ spectrum.

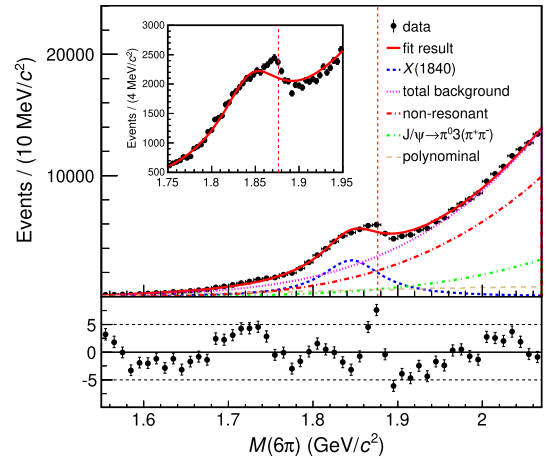


FIG. 2. Fit result of the $M(6\pi)$ distribution with a simple BW function. The dots with error bars are data, the solid curve in red is the total fit result, the dashed line in blue is the $X(1840)$ signal, the dash-dotted line in green is the background events from $J/\psi \rightarrow \pi^0 3(\pi^+\pi^-)$, and the dotted line in magenta is the sum of background.

To resolve the discrepancy from data, two different models for the line shape of the structure around $1.84 \text{ GeV}/c^2$ are applied to investigate the resonances in the $M(6\pi)$ spectrum. With an assumption of the line shape of $3(\pi^+\pi^-)$ above the $p\bar{p}$ mass threshold affected by the opening of the $X(1840) \rightarrow p\bar{p}$ decay (model I), we try to describe the anomalous shape with a Flatté formula [33],

$$A = \left| \frac{1}{M^2 - s - i\sum_j g_j^2 \rho_j} \right|^2,$$

where M is a parameter with the dimension of mass, s is the mass square of the $3(\pi^+\pi^-)$ combination, ρ_j is the phase space for the decay mode j , and g_j^2 is the corresponding coupling strength. The $\sum_j g_j^2 \rho_j$ term describes how the decay width varies with s . Approximately,

$$\sum_j g_j^2 \rho_j \approx g_0^2 \left(\rho_0 + \frac{g_{p\bar{p}}^2}{g_0^2} \rho_{p\bar{p}} \right), \quad (1)$$

where g_0^2 is the sum of g^2 of all decay modes other than $X(1840) \rightarrow p\bar{p}$, ρ_0 is the maximum two-body decay phase space volume [29], and $g_{p\bar{p}}^2/g_0^2$ is the ratio between the coupling strength to the $p\bar{p}$ channel and the sum of all other channels. This fit, as illustrated in Fig. 3(a), yields $M = 1.818 \pm 0.009 \text{ GeV}/c^2$, $g_0^2 = 18.0 \pm 2.8 \text{ GeV}^2/c^4$, and $g_{p\bar{p}}^2 = 51.4 \pm 14.8 \text{ GeV}^2/c^4$. This model fit has a $\log \mathcal{L}$ that is improved over the simple Breit-Wigner one by 42.8. The significance of $g_{p\bar{p}}^2/g_0^2$ being nonzero is 9.2σ . The goodness of the fit $\chi^2/N_{\text{dof}} = 317.9/44$, yet not enough to be acceptable for a good description of data.

A comparison between the fit result of model I and the data reveals a tension around the $p\bar{p}$ mass threshold. To obtain a better description on data, another model allows for interference between two resonant components (model II) and the coherent sum of them is defined as

$$A = \left| \frac{1}{M_1^2 - s - iM_1\Gamma_1} + \beta \frac{1}{M_2^2 - s - iM_2\Gamma_2} \right|^2, \quad (2)$$

where M_1, Γ_1, M_2 , and Γ_2 represent the masses and widths of the two resonant structures, denoted as $X(1840)$ and $X(1880)$, respectively. β is a complex parameter accounting for the contribution of $X(1880)$ relative to the $X(1840)$ as well as the phase between them.

The fit with model II improves the fit quality significantly ($\chi^2/N_{\text{dof}} = 155.6/41$), in particular for the region around the $p\bar{p}$ mass threshold, which is illustrated in Fig. 3(b). The χ^2 value in the region of 1.78 to $1.92 \text{ GeV}/c^2$ changes from 135.6 for model I to 15.1 for model II, which shows the latter model provides a significant improvement in describing the anomalous line shape. The masses, widths, and signal yields of these two

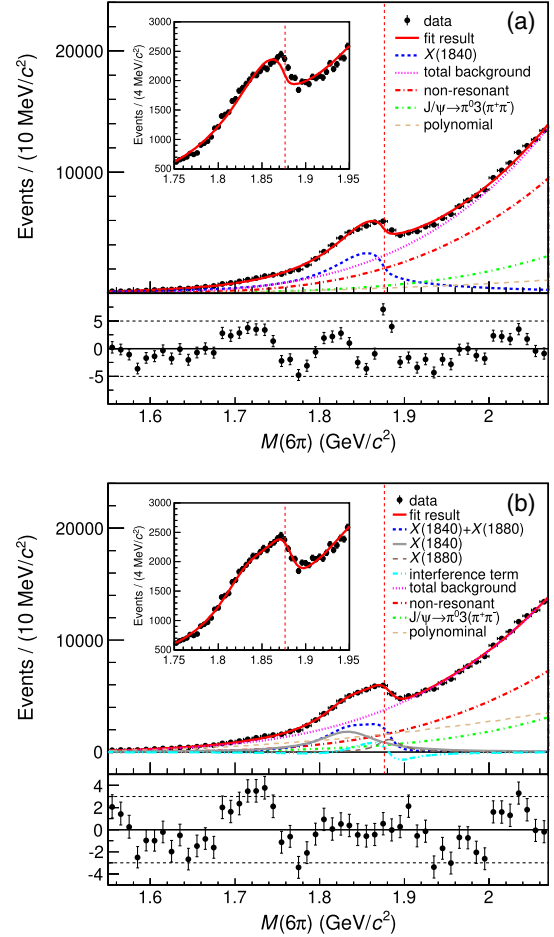


FIG. 3. Fit result of the $M(6\pi)$ distribution with model I (a), and solution I for the model II (b). The dashed line in blue is the $X(1840)$ signal for (a), and the sum of $X(1840)$ and $X(1880)$ for (b).

resonant components, as summarized in Table I, are determined to be $M_{X(1840)} = 1832.5 \pm 3.1 \text{ MeV}/c^2$, $\Gamma_{X(1840)} = 80.7 \pm 5.2 \text{ MeV}$, $N_{X(1840)} = 20980 \pm 5341$, $M_{X(1880)} = 1882.1 \pm 1.7 \text{ MeV}/c^2$, $\Gamma_{X(1880)} = 30.7 \pm 5.5 \text{ MeV}$, $N_{X(1880)} = 5460 \pm 3757$, where the uncertainties are statistical only. The $\log \mathcal{L}$ of this fit is improved by 73.6 over that of the fit with model I. The statistical significance of $X(1880)$ is found to be larger than 10σ , which is determined by comparing the log-likelihood value and the number of degrees of freedom between model II and model I using Wilks' theorem [34]. As discussed in Ref. [35], a fit using a coherent sum of two BW functions may result in two nontrivial solutions with the same resonant parameters. We make an extensive investigation on the fit and find the second solution with the same fit quality, which yields $N_{X(1840)} = 36506 \pm 8740$ and $N_{X(1880)} = 22097 \pm 5794$, corresponding to the destructive interference as described in Ref. [35]. The figure of second solution is given in Supplemental Material [36].

TABLE I. The fitted parameters of the two coherent resonant structures and the corresponding product branching fractions. Solutions I and II refer to the solutions characterizing model II as discussed in the text.

Parameters	Solution I	Solution II
$M_{X(1840)}$ (MeV/ c^2)	$1832.5 \pm 3.1 \pm 2.5$	
$\Gamma_{X(1840)}$ (MeV)	$80.7 \pm 5.2 \pm 7.7$	
$\mathcal{B}_{X(1840)} (\times 10^{-5})$	$1.19 \pm 0.30 \pm 0.15$	$2.07 \pm 0.50 \pm 0.36$
$M_{X(1880)}$ (MeV/ c^2)	$1882.1 \pm 1.7 \pm 0.7$	
$\Gamma_{X(1880)}$ (MeV)	$30.7 \pm 5.5 \pm 2.4$	
$\mathcal{B}_{X(1880)} (\times 10^{-5})$	$0.29 \pm 0.20 \pm 0.09$	$1.19 \pm 0.31 \pm 0.18$

Since the $X(1835)$ is known as a pseudoscalar meson, the $X(1840)$ is supposed to be a pseudoscalar particle as well considering the similar behaviors with those of the $X(1835)$. For the radiative J/ψ decay to a pseudoscalar meson, the polar angle of the photon in the J/ψ rest frame, denoted as θ , is expected to follow a $1 + \cos^2 \theta$ distribution. The $|\cos \theta|$ is divided into nine bins in a region of $[0, 0.9]$ to investigate the angular distribution. The number of signal events corresponding to the constructive interference solution in each bin is obtained with the same fit procedure as mentioned above. The result is shown in Fig. 4. As a result, the angular distributions of $X(1840)$ and $X(1880)$ both agree with $1 + \cos^2 \theta$ and support the interpretation of the pseudoscalar mesons. With the hypotheses of pseudoscalar mesons, the detection efficiencies for $J/\psi \rightarrow \gamma X(1840)$ and $J/\psi \rightarrow \gamma X(1880)$, 17.4% and 18.4%, are obtained from the MC simulation. The product branching fractions corresponding to those two solutions are summarized in Table I.

Sources of systematic uncertainties and their corresponding contributions to the measurement of the branching fractions are summarized in Table II. The uncertainties

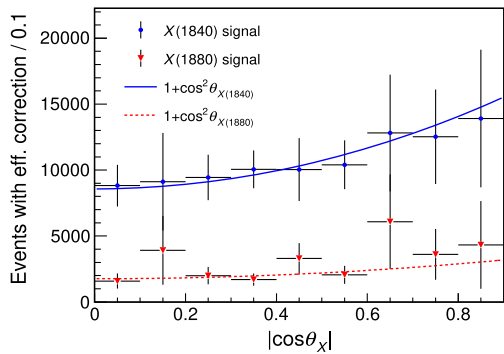


FIG. 4. The acceptance-corrected angular distribution with respect to $|\cos \theta|$ for the $X(1840)$ and $X(1880)$, respectively. The curves represent the fit results with the function of $1 + \cos^2 \theta$ to the above two components: the solid curve in blue is for the $X(1840)$; the dashed one in red is for the $X(1880)$.

TABLE II. Relative systematic uncertainties in the product branching fractions (in percent).

Sources	$X(1840)$	$X(1880)$
MDC tracking	6.0	6.0
Photon detection	1.0	1.0
Kinematic fit	0.6	0.6
Detection efficiency	3.0	3.1
Number of J/ψ events	0.4	0.4
Background uncertainty (Solution I)	10.0	27.8
Background uncertainty (Solution II)	16.1	12.9
Total (Solution I)	12.1	28.6
Total (Solution II)	17.5	14.6

come from data-MC differences (tracking, photon detection, 4C kinematic fit, etc.), total number of J/ψ events, and background uncertainty from the change of fit range, MC model, MC statistics. For the MC model uncertainties due to the unknown spin parity of the structures, we use the difference between phase space and a pseudoscalar meson hypothesis. In accordance with the previous publication [37], we keep the efficiency with the track helix correction as the nominal value in this Letter, and take the difference between the efficiencies with and without correction as the systematic uncertainty from the 4C kinematic fit. The main contribution of systematic uncertainty comes from the uncertainty in the background estimation which is accessed by changing fit ranges. The uncertainty caused by the contribution above 2.07 GeV of the $M(6\pi)$ spectrum has a considerable effect on the parametrization of the remaining background, which results in a large uncertainty of the branching fractions. Meanwhile, the impact of this uncertainty on the statistical significance of $X(1880)$ is considered, and the smallest statistical significance is chosen as the final result. The total systematic uncertainty is obtained by adding all of the mentioned ones in quadrature under the assumption that they are independent. The total systematic uncertainties on mass and width are estimated from the background uncertainty due to fit range and background description, and found to be ± 2.5 MeV/ c^2 and ± 7.7 MeV for the $X(1840)$, ± 0.7 MeV/ c^2 and ± 2.4 MeV for the $X(1880)$, respectively. Since the mass resolution of 4 MeV/ c^2 is much smaller than the width of these structures, the uncertainty from the detector resolution is found to be negligible. The final results given in Table I are obtained considering all the systematic uncertainties reported in Table II.

In summary, a study of the radiative decay $J/\psi \rightarrow \gamma 3(\pi^+ \pi^-)$ is performed with a sample of $(10087 \pm 44) \times 10^6$ J/ψ events accumulated at the BESIII detector. A significant distortion of the $M(6\pi)$ distribution near the $p\bar{p}$ mass threshold is observed for the first time, which is analogous to the distortion observed in the $\pi^+ \pi^- \eta'$ invariant mass spectrum in $J/\psi \rightarrow \gamma \pi^+ \pi^- \eta'$ [17].

To understand this anomalous line shape, a few interpretations including a single structure described by a single BW function or with threshold effect (model I) and a coherent sum of two structures (model II) are tested. We find that neither a simple BW function nor a Flatté function could provide a reasonable description of data. The scheme of a coherent sum of two structures gives a much better description on the anomalous line shape in the $M(6\pi)$ spectrum. According to the fit results, the narrow structure $X(1880)$ has a mass of $M = 1882.1 \pm 1.7 \pm 0.7 \text{ MeV}/c^2$ and a width of $\Gamma = 30.7 \pm 5.5 \pm 2.4 \text{ MeV}$. The significance of $X(1880)$ is larger than 10σ compared to the fit result with model I considering any effect associated to the systematic uncertainties. The mass and width of $X(1840)$ are measured to be $M = 1832.5 \pm 3.1 \pm 2.5 \text{ MeV}/c^2$ and $\Gamma = 80.7 \pm 5.2 \pm 7.7 \text{ MeV}$, which are in agreement with the previous work [16]. Two solutions with the same fit quality and the identical resonant parameters but different branching fractions due to the constructive or destructive interference are summarized in Table I.

Compared with the two structures observed in the $M(\pi^+\pi^-\eta')$ spectrum [17], the $X(1840)$ has a consistent mass with that $X(1835)$ but much narrower width. The mass and width of the $X(1880)$ obtained in this Letter are in reasonable agreement with those reported in Ref. [17], which are $1870.2 \pm 2.2^{+2.3}_{-0.7} \text{ MeV}/c^2$ and $13.0 \pm 6.1^{+2.1}_{-3.8} \text{ MeV}$, respectively. This further supports the existence of a $p\bar{p}$ bound state just spanning the $p\bar{p}$ mass threshold. At present, more sophisticated parametrizations such as a mixture of above two models cannot be ruled out. The observed anomalous line shape in the $M(6\pi)$ spectrum in $J/\psi \rightarrow \gamma 3(\pi^+\pi^-)$ and the $\pi^+\pi^-\eta'$ invariant mass spectrum in $J/\psi \rightarrow \gamma \pi^+\pi^-\eta'$ reveal complex resonant structures near the $p\bar{p}$ mass threshold. To establish the relationship between different resonances in the mass region of $[1.8, 1.9] \text{ GeV}/c^2$ and determine the nature of the underlying resonant structures, more data along with additional measurements including the determination of the spin-parity quantum numbers and the coupled channel amplitude analysis are highly desirable.

The BESIII Collaboration thanks the staff of BEPCII and the IHEP computing center for their strong support. This work is supported in part by National Key R&D Program of China under Contracts No. 2020YFA0406300, No. 2020YFA0406400; National Natural Science Foundation of China (NSFC) under Contracts No. 11635010, No. 11735014, No. 11835012, No. 11905037, No. 11935015, No. 11935016, No. 11935018, No. 11961141012, No. 12022510, No. 12025502, No. 12035009, No. 12035013, No. 12061131003, No. 12192260, No. 12192261, No. 12192262, No. 12192263, No. 12192264, No. 12192265, No. 12221005, No. 12225509, No. 12235017; the Chinese Academy of Sciences (CAS)

Large-Scale Scientific Facility Program; the CAS Center for Excellence in Particle Physics (CCEPP); Joint Large-Scale Scientific Facility Funds of the NSFC and CAS under Contract No. U1832207; CAS Key Research Program of Frontier Sciences under Contracts No. QYZDJ-SSW-SLH003, No. QYZDJ-SSW-SLH040; 100 Talents Program of CAS; The Institute of Nuclear and Particle Physics (INPAC) and Shanghai Key Laboratory for Particle Physics and Cosmology; ERC under Contract No. 758462; European Union's Horizon 2020 research and innovation programme under Marie Skłodowska-Curie grant agreement under Contract No. 894790; German Research Foundation DFG under Contract No. 455635585, Collaborative Research Center CRC 1044, FOR5327, GRK 2149; Istituto Nazionale di Fisica Nucleare, Italy; Ministry of Development of Turkey under Contract No. DPT2006K-120470; National Research Foundation of Korea under Contract No. NRF-2022R1A2C1092335; National Science and Technology fund of Mongolia; National Science Research and Innovation Fund (NSRF) via the Program Management Unit for Human Resources & Institutional Development, Research and Innovation of Thailand under Contract No. B16F640076; Polish National Science Centre under Contract No. 2019/35/O/ST2/02907; The Swedish Research Council; U.S. Department of Energy under Contract No. DE-FG02-05ER41374.

-
- [1] M. Ablikim *et al.* (BES Collaboration), *Phys. Rev. Lett.* **95**, 262001 (2005).
 - [2] J. Z. Bai *et al.* (BES Collaboration), *Phys. Rev. Lett.* **91**, 022001 (2003).
 - [3] J. P. Dedonder, B. Loiseau, B. El-Bennich, and S. Wycech, *Phys. Rev. C* **80**, 045207 (2009).
 - [4] X.-H. Liu, Y.-J. Zhang, and Q. Zhao, *Phys. Rev. D* **80**, 034032 (2009).
 - [5] G.-J. Ding and M.-L. Yan, *Eur. Phys. J. A* **28**, 351 (2006).
 - [6] Z.-G. Wang and S.-L. Wan, *J. Phys. G* **34**, 505 (2007).
 - [7] B. A. Li, *Phys. Rev. D* **74**, 034019 (2006).
 - [8] N. Kochelev and D.-P. Min, *Phys. Lett. B* **633**, 283 (2006).
 - [9] G. Hao, C.-F. Qiao, and A.-L. Zhang, *Phys. Lett. B* **642**, 53 (2006).
 - [10] T. Huang and S.-L. Zhu, *Phys. Rev. D* **73**, 014023 (2006).
 - [11] M. Ablikim *et al.* (BESIII Collaboration), *Chin. Phys. C* **34**, 421 (2010).
 - [12] M. Ablikim *et al.* (BESIII Collaboration), *Phys. Rev. Lett.* **106**, 072002 (2011).
 - [13] J. P. Alexander *et al.* (CLEO Collaboration), *Phys. Rev. D* **82**, 092002 (2010).
 - [14] M. Ablikim *et al.* (BESIII Collaboration), *Phys. Rev. Lett.* **108**, 112003 (2012).
 - [15] M. Ablikim *et al.* (BESIII Collaboration), *Phys. Rev. Lett.* **115**, 091803 (2015).
 - [16] M. Ablikim *et al.* (BESIII Collaboration), *Phys. Rev. D* **88**, 091502 (2013).

- [17] M. Ablikim *et al.* (BESIII Collaboration), *Phys. Rev. Lett.* **117**, 042002 (2016).
- [18] M. Ablikim *et al.* (BESIII Collaboration), *Chin. Phys. C* **46**, 074001 (2022).
- [19] C. Yu *et al.*, in *Proceedings of International Particle Accelerator Conference (IPAC'16), Busan, Korea, 2016*, International Particle Accelerator Conference No. 7 (JA-CoW, Geneva, Switzerland, 2016), pp. 1014–1018.
- [20] M. Ablikim *et al.* (BESIII Collaboration), *Nucl. Instrum. Methods Phys. Res., Sect. A* **614**, 345 (2010).
- [21] X. Li *et al.*, *Radiat. Detect. Technol. Methods* **1**, 13 (2017).
- [22] Y.-X. Guo, S.-S. Sun, F.-F. An, R.-X. Yang, M. Zhou, Z. Wu, H.-L. Dai, Y.-K. Heng, C. Li, Z.-Y. Deng, H.-M. Liu, and W.-G. Li, *Radiat. Detect. Technol. Methods* **1**, 15 (2017).
- [23] P. Cao *et al.*, *Nucl. Instrum. Methods Phys. Res., Sect. A* **953**, 163053 (2020).
- [24] S. Agostinelli *et al.* (GEANT4 Collaboration), *Nucl. Instrum. Methods Phys. Res., Sect. A* **506**, 250 (2003).
- [25] K.-X. Huang, Z.-J. Li, Z. Qian, J. Zhu, H.-Y. Li, Y.-M. Zhang, S.-S. Sun, and Z.-Y. You, *Nucl. Sci. Tech.* **33**, 142 (2022).
- [26] S. Jadach, B. F. L. Ward, and Z. Was, *Phys. Rev. D* **63**, 113009 (2001).
- [27] D. J. Lange, *Nucl. Instrum. Methods Phys. Res., Sect. A* **462**, 152 (2001).
- [28] R.-G. Ping, *Chin. Phys. C* **32**, 599 (2008).
- [29] R. L. Workman *et al.* (Particle Data Group), *Prog. Theor. Exp. Phys.* **2022**, 083C01 (2022).
- [30] J. C. Chen, G. S. Huang, X. R. Qi, D. H. Zhang, and Y. S. Zhu, *Phys. Rev. D* **62**, 034003 (2000).
- [31] R.-L. Yang, R.-G. Ping, and H. Chen, *Chin. Phys. Lett.* **31**, 061301 (2014).
- [32] E. Richter-Was, *Phys. Lett. B* **303**, 163 (1993).
- [33] S. M. Flatte, *Phys. Lett.* **63B**, 224 (1976).
- [34] S. S. Wilks, *Ann. Math. Stat.* **9**, 60 (1938).
- [35] K. Zhu, X. H. Mo, C. Z. Yuan, and P. Wang, *Int. J. Mod. Phys. A* **26**, 4511 (2011).
- [36] See Supplemental Material at <http://link.aps.org/supplemental/10.1103/PhysRevLett.132.151901> for the figure of solution II.
- [37] M. Ablikim *et al.* (BESIII Collaboration), *Phys. Rev. D* **87**, 012002 (2013).

M. Ablikim,¹ M. N. Achasov,^{5,b} P. Adlarson,⁷⁵ X. C. Ai,⁸¹ R. Aliberti,³⁶ A. Amoroso,^{74a,74c} M. R. An,⁴⁰ Q. An,^{71,58} Y. Bai,⁵⁷ O. Bakina,³⁷ I. Balossino,^{30a} Y. Ban,^{47,g} V. Batozskaya,^{1,45} K. Begzsuren,³³ N. Berger,³⁶ M. Berlowski,⁴⁵ M. Bertani,^{29a} D. Bettoni,^{30a} F. Bianchi,^{74a,74c} E. Bianco,^{74a,74c} A. Bortone,^{74a,74c} I. Boyko,³⁷ R. A. Briere,⁶ A. Brueggemann,⁶⁸ H. Cai,⁷⁶ X. Cai,^{1,58} A. Calcaterra,^{29a} G. F. Cao,^{1,63} N. Cao,^{1,63} S. A. Cetin,^{62a} J. F. Chang,^{1,58} T. T. Chang,⁷⁷ W. L. Chang,^{1,63} G. R. Che,⁴⁴ G. Chelkov,^{37,a} C. Chen,⁴⁴ Chao Chen,⁵⁵ G. Chen,¹ H. S. Chen,^{1,63} M. L. Chen,^{1,58,63} S. J. Chen,⁴³ S. L. Chen,⁴⁶ S. M. Chen,⁶¹ T. Chen,^{1,63} X. R. Chen,^{32,63} X. T. Chen,^{1,63} Y. B. Chen,^{1,58} Y. Q. Chen,³⁵ Z. J. Chen,^{26,h} W. S. Cheng,^{74c} S. K. Choi,¹¹ X. Chu,⁴⁴ G. Cibinetto,^{30a} S. C. Coen,⁴ F. Cossio,^{74c} J. J. Cui,⁵⁰ H. L. Dai,^{1,58} J. P. Dai,⁷⁹ A. Dbeyssi,¹⁹ R. E. de Boer,⁴ D. Dedovich,³⁷ Z. Y. Deng,¹ A. Denig,³⁶ I. Denysenko,³⁷ M. Destefanis,^{74a,74c} F. De Mori,^{74a,74c} B. Ding,^{66,1} X. X. Ding,^{47,g} Y. Ding,³⁵ Y. Ding,⁴¹ J. Dong,^{1,58} L. Y. Dong,^{1,63} M. Y. Dong,^{1,58,63} X. Dong,⁷⁶ M. C. Du,¹ S. X. Du,⁸¹ Z. H. Duan,⁴³ P. Egorov,^{37,a} Y. H. Fan,⁴⁶ Y. L. Fan,⁷⁶ J. Fang,^{1,58} S. S. Fang,^{1,63} W. X. Fang,¹ Y. Fang,¹ R. Farinelli,^{30a} L. Fava,^{74b,74c} F. Feldbauer,⁴ G. Felici,^{29a} C. Q. Feng,^{71,58} J. H. Feng,⁵⁹ K. Fischer,⁶⁹ M. Fritsch,⁴ C. Fritsch,⁶⁸ C. D. Fu,¹ J. L. Fu,⁶³ Y. W. Fu,¹ H. Gao,⁶³ Y. N. Gao,^{47,g} Yang Gao,^{71,58} S. Garbolino,^{74c} I. Garzia,^{30a,30b} P. T. Ge,⁷⁶ Z. W. Ge,⁴³ C. Geng,⁵⁹ E. M. Gersabeck,⁶⁷ A. Gilman,⁶⁹ K. Goetzen,¹⁴ L. Gong,⁴¹ W. X. Gong,^{1,58} W. Gradl,³⁶ S. Gramigna,^{30a,30b} M. Greco,^{74a,74c} M. H. Gu,^{1,58} Y. T. Gu,¹⁶ C. Y. Guan,^{1,63} Z. L. Guan,²³ A. Q. Guo,^{32,63} L. B. Guo,⁴² M. J. Guo,⁵⁰ R. P. Guo,⁴⁹ Y. P. Guo,^{13,f} A. Guskov,^{37,a} T. T. Han,⁵⁰ W. Y. Han,⁴⁰ X. Q. Hao,²⁰ F. A. Harris,⁶⁵ K. K. He,⁵⁵ K. L. He,^{1,63} F. H. H. Heinsius,⁴ C. H. Heinz,³⁶ Y. K. Heng,^{1,58,63} C. Herold,⁶⁰ T. Holtmann,⁴ P. C. Hong,^{13,f} G. Y. Hou,^{1,63} X. T. Hou,^{1,63} Y. R. Hou,⁶³ Z. L. Hou,¹ H. M. Hu,^{1,63} J. F. Hu,^{56,i} T. Hu,^{1,58,63} Y. Hu,¹ G. S. Huang,^{71,58} K. X. Huang,⁵⁹ L. Q. Huang,^{32,63} X. T. Huang,⁵⁰ Y. P. Huang,¹ T. Hussain,⁷³ N. Hüsken,^{28,36} W. Imoehl,²⁸ N. in der Wiesche,⁶⁸ J. Jackson,²⁸ S. Jaeger,⁴ S. Janchiv,³³ J. H. Jeong,¹¹ Q. Ji,¹ Q. P. Ji,²⁰ X. B. Ji,^{1,63} X. L. Ji,^{1,58} Y. Y. Ji,⁵⁰ X. Q. Jia,⁵⁰ Z. K. Jia,^{71,58} H. J. Jiang,⁷⁶ P. C. Jiang,^{47,g} S. S. Jiang,⁴⁰ T. J. Jiang,¹⁷ X. S. Jiang,^{1,58,63} Y. Jiang,⁶³ J. B. Jiao,⁵⁰ Z. Jiao,²⁴ S. Jin,⁴³ Y. Jin,⁶⁶ M. Q. Jing,^{1,63} T. Johansson,⁷⁵ S. Kabana,³⁴ N. Kalantar-Nayestanaki,⁶⁴ X. L. Kang,¹⁰ X. S. Kang,⁴¹ M. Kavatsyuk,⁶⁴ B. C. Ke,⁸¹ A. Khoukaz,⁶⁸ R. Kiuchi,¹ R. Kliemt,¹⁴ O. B. Kolcu,^{62a} B. Kopf,⁴ M. Kuessner,⁴ X. Kui,¹ A. Kupsc,^{45,75} W. Kühn,³⁸ J. J. Lane,⁶⁷ P. Larin,¹⁹ A. Lavania,²⁷ L. Lavezzi,^{74a,74c} T. T. Lei,^{71,58} Z. H. Lei,^{71,58} H. Leithoff,³⁶ M. Lellmann,³⁶ T. Lenz,³⁶ C. Li,⁴⁸ C. Li,⁴⁴ C. H. Li,⁴⁰ Cheng Li,^{71,58} D. M. Li,⁸¹ F. Li,^{1,58} G. Li,¹ H. Li,^{71,58} H. B. Li,^{1,63} H. J. Li,²⁰ H. N. Li,^{56,i} Hui Li,⁴⁴ J. R. Li,⁶¹ J. S. Li,⁵⁹ J. W. Li,⁵⁰ K. L. Li,²⁰ Ke Li,¹ L. J. Li,^{1,63} L. K. Li,¹ Lei Li,³ M. H. Li,⁴⁴ P. R. Li,^{39,j,k} Q. X. Li,⁵⁰ S. X. Li,¹³ T. Li,⁵⁰ W. D. Li,^{1,63} W. G. Li,¹ X. H. Li,^{71,58} X. L. Li,⁵⁰ Xiaoyu Li,^{1,63} Y. G. Li,^{47,g} Z. J. Li,⁵⁹ Z. X. Li,¹⁶ C. Liang,⁴³ H. Liang,^{71,58} H. Liang,^{1,63} H. Liang,³⁵ Y. F. Liang,⁵⁴ Y. T. Liang,^{32,63} G. R. Liao,¹⁵ L. Z. Liao,⁵⁰ Y. P. Liao,^{1,63} J. Libby,²⁷ A. Limphirat,⁶⁰ D. X. Lin,^{32,63} T. Lin,¹ B. J. Liu,¹ B. X. Liu,⁷⁶ C. Liu,³⁵ C. X. Liu,¹ F. H. Liu,⁵³ Fang Liu,¹ Feng Liu,⁷ G. M. Liu,^{56,i} H. Liu,^{39,j,k} H. B. Liu,¹⁶ H. M. Liu,^{1,63} Huanhuan Liu,¹ Huihui Liu,²² J. B. Liu,^{71,58} J. L. Liu,⁷² J. Y. Liu,^{1,63}

K. Liu,¹ K. Y. Liu,⁴¹ Ke Liu,²³ L. Liu,^{71,58} L. C. Liu,⁴⁴ Lu Liu,⁴⁴ M. H. Liu,^{13,f} P. L. Liu,¹ Q. Liu,⁶³ S. B. Liu,^{71,58} T. Liu,^{13,f} W. K. Liu,⁴⁴ W. M. Liu,^{71,58} X. Liu,^{39,j,k} Y. Liu,⁸¹ Y. Liu,^{39,j,k} Y. B. Liu,⁴⁴ Z. A. Liu,^{1,58,63} Z. Q. Liu,⁵⁰ X. C. Lou,^{1,58,63} F. X. Lu,⁵⁹ H. J. Lu,²⁴ J. G. Lu,^{1,58} X. L. Lu,¹ Y. Lu,⁸ Y. P. Lu,^{1,58} Z. H. Lu,^{1,63} C. L. Luo,⁴² M. X. Luo,⁸⁰ T. Luo,^{13,f} X. L. Luo,^{1,58} X. R. Lyu,⁶³ Y. F. Lyu,⁴⁴ F. C. Ma,⁴¹ H. L. Ma,¹ J. L. Ma,^{1,63} L. L. Ma,⁵⁰ M. M. Ma,^{1,63} Q. M. Ma,¹ R. Q. Ma,^{1,63} R. T. Ma,⁶³ X. Y. Ma,^{1,58} Y. Ma,^{47,g} Y. M. Ma,³² F. E. Maas,¹⁹ M. Maggiora,^{74a,74c} S. Malde,⁶⁹ Q. A. Malik,⁷³ A. Mangoni,^{29b} Y. J. Mao,^{47,g} Z. P. Mao,¹ S. Marcello,^{74a,74c} Z. X. Meng,⁶⁶ J. G. Messchendorp,^{14,64} G. Mezzadri,^{30a} H. Miao,^{1,63} T. J. Min,⁴³ R. E. Mitchell,²⁸ X. H. Mo,^{1,58,63} N. Yu. Muchnoi,^{5,b} J. Muskalla,³⁶ Y. Nefedov,³⁷ F. Nerling,^{19,d} I. B. Nikolaev,^{5,b} Z. Ning,^{1,58} S. Nisar,^{12,1} W. D. Niu,⁵⁵ Y. Niu,⁵⁰ S. L. Olsen,⁶³ Q. Ouyang,^{1,58,63} S. Pacetti,^{29b,29c} X. Pan,⁵⁵ Y. Pan,⁵⁷ A. Pathak,³⁵ P. Patteri,^{29a} Y. P. Pei,^{71,58} M. Pelizaeus,⁴ H. P. Peng,^{71,58} K. Peters,^{14,d} J. L. Ping,⁴² R. G. Ping,^{1,63} S. Plura,³⁶ S. Pogodin,³⁷ V. Prasad,³⁴ F. Z. Qi,¹ H. Qi,^{71,58} H. R. Qi,⁶¹ M. Qi,⁴³ T. Y. Qi,^{13,f} S. Qian,^{1,58} W. B. Qian,⁶³ C. F. Qiao,⁶³ J. J. Qin,⁷² L. Q. Qin,¹⁵ X. P. Qin,^{13,f} X. S. Qin,⁵⁰ Z. H. Qin,^{1,58} J. F. Qiu,¹ S. Q. Qu,⁶¹ C. F. Redmer,³⁶ K. J. Ren,⁴⁰ A. Rivetti,^{74c} M. Rolo,^{74c} G. Rong,^{1,63} Ch. Rosner,¹⁹ S. N. Ruan,⁴⁴ N. Salone,⁴⁵ A. Sarantsev,^{37,c} Y. Schelhaas,³⁶ K. Schoenning,⁷⁵ M. Scodreggio,^{30a,30b} K. Y. Shan,^{13,f} W. Shan,²⁵ X. Y. Shan,^{71,58} J. F. Shangguan,⁵⁵ L. G. Shao,^{1,63} M. Shao,^{71,58} C. P. Shen,^{13,f} H. F. Shen,^{1,63} W. H. Shen,⁶³ X. Y. Shen,^{1,63} B. A. Shi,⁶³ H. C. Shi,^{71,58} J. L. Shi,¹³ J. Y. Shi,¹ Q. Q. Shi,⁵⁵ R. S. Shi,^{1,63} X. Shi,^{1,58} J. J. Song,²⁰ T. Z. Song,⁵⁹ W. M. Song,^{35,1} Y. J. Song,¹³ Y. X. Song,^{47,g} S. Sosio,^{74a,74c} S. Spataro,^{74a,74c} F. Stieler,³⁶ Y. J. Su,⁶³ G. B. Sun,⁷⁶ G. X. Sun,¹ H. Sun,⁶³ H. K. Sun,¹ J. F. Sun,²⁰ K. Sun,⁶¹ L. Sun,⁷⁶ S. S. Sun,^{1,63} T. Sun,^{1,63} W. Y. Sun,³⁵ Y. Sun,¹⁰ Y. J. Sun,^{71,58} Y. Z. Sun,¹ Z. T. Sun,⁵⁰ Y. X. Tan,^{71,58} C. J. Tang,⁵⁴ G. Y. Tang,¹ J. Tang,⁵⁹ Y. A. Tang,⁷⁶ L. Y. Tao,⁷² Q. T. Tao,^{26,h} M. Tat,⁶⁹ J. X. Teng,^{71,58} V. Thoren,⁷⁵ W. H. Tian,⁵⁹ W. H. Tian,⁵² Y. Tian,^{32,63} Z. F. Tian,⁷⁶ I. Uman,^{62b} S. J. Wang,⁵⁰ B. Wang,¹ B. L. Wang,⁶³ Bo Wang,^{71,58} C. W. Wang,⁴³ D. Y. Wang,^{47,g} F. Wang,⁷² H. J. Wang,^{39,j,k} H. P. Wang,^{1,63} J. P. Wang,⁵⁰ K. Wang,^{1,58} L. L. Wang,¹ M. Wang,⁵⁰ Meng Wang,^{1,63} S. Wang,^{39,j,k} S. Wang,^{13,f} T. Wang,^{13,f} T. J. Wang,⁴⁴ W. Wang,⁷² W. Wang,⁵⁹ W. P. Wang,^{71,58} X. Wang,^{47,g} X. F. Wang,^{39,j,k} X. J. Wang,⁴⁰ X. L. Wang,^{13,f} Y. Wang,⁶¹ Y. D. Wang,⁴⁶ Y. F. Wang,^{1,58,63} Y. H. Wang,⁴⁸ Y. N. Wang,⁴⁶ Y. Q. Wang,¹ Yaqian Wang,^{18,1} Yi Wang,⁶¹ Z. Wang,^{1,58} Z. L. Wang,⁷² Z. Y. Wang,^{1,63} Ziyi Wang,⁶³ D. Wei,⁷⁰ D. H. Wei,¹⁵ F. Weidner,⁶⁸ S. P. Wen,¹ C. W. Wenzel,⁴ U. Wiedner,⁴ G. Wilkinson,⁶⁹ M. Wolke,⁷⁵ L. Wollenberg,⁴ C. Wu,⁴⁰ J. F. Wu,^{1,63} L. H. Wu,¹ L. J. Wu,^{1,63} X. Wu,^{13,f} X. H. Wu,³⁵ Y. Wu,⁷¹ Y. H. Wu,⁵⁵ Y. J. Wu,³² Z. Wu,^{1,58} L. Xia,^{71,58} X. M. Xian,⁴⁰ T. Xiang,^{47,g} D. Xiao,^{39,j,k} G. Y. Xiao,⁴³ S. Y. Xiao,¹ Y. L. Xiao,^{13,f} Z. J. Xiao,⁴² C. Xie,⁴³ X. H. Xie,^{47,g} Y. Xie,⁵⁰ Y. G. Xie,^{1,58} Y. H. Xie,⁷ Z. P. Xie,^{71,58} T. Y. Xing,^{1,63} C. F. Xu,^{1,63} C. J. Xu,⁵⁹ G. F. Xu,¹ H. Y. Xu,⁶⁶ Q. J. Xu,¹⁷ Q. N. Xu,⁸¹ W. Xu,^{1,63} W. L. Xu,⁶⁶ X. P. Xu,⁵⁵ Y. C. Xu,⁷⁸ Z. P. Xu,⁴³ Z. S. Xu,⁶³ F. Yan,^{13,f} L. Yan,^{13,f} W. B. Yan,^{71,58} W. C. Yan,⁸¹ X. Q. Yan,¹ H. J. Yang,^{51,e} H. L. Yang,³⁵ H. X. Yang,¹ Tao Yang,¹ Y. Yang,^{13,f} Y. F. Yang,⁴⁴ Y. X. Yang,^{1,63} Yifan Yang,^{1,63} Z. W. Yang,^{39,j,k} Z. P. Yao,⁵⁰ M. Ye,^{1,58} M. H. Ye,⁹ J. H. Yin,¹ Z. Y. You,⁵⁹ B. X. Yu,^{1,58,63} C. X. Yu,⁴⁴ G. Yu,^{1,63} J. S. Yu,^{26,h} T. Yu,⁷² X. D. Yu,^{47,g} C. Z. Yuan,^{1,63} L. Yuan,² S. C. Yuan,¹ X. Q. Yuan,¹ Y. Yuan,^{1,63} Z. Y. Yuan,⁵⁹ C. X. Yue,⁴⁰ A. A. Zafar,⁷³ F. R. Zeng,⁵⁰ X. Zeng,^{13,f} Y. Zeng,^{26,h} Y. J. Zeng,^{1,63} X. Y. Zhai,³⁵ Y. C. Zhai,⁵⁰ Y. H. Zhan,⁵⁹ A. Q. Zhang,^{1,63} B. L. Zhang,^{1,63} B. X. Zhang,¹ D. H. Zhang,⁴⁴ G. Y. Zhang,²⁰ H. Zhang,⁷¹ H. H. Zhang,⁵⁹ H. H. Zhang,³⁵ H. Q. Zhang,^{1,58,63} H. Y. Zhang,^{1,58} J. Zhang,⁸¹ J. J. Zhang,⁵² J. L. Zhang,²¹ J. Q. Zhang,⁴² J. W. Zhang,^{1,58,63} J. X. Zhang,^{39,j,k} J. Y. Zhang,¹ J. Z. Zhang,^{1,63} Jianyu Zhang,⁶³ Jiawei Zhang,^{1,63} L. M. Zhang,⁶¹ L. Q. Zhang,⁵⁹ Lei Zhang,⁴³ P. Zhang,^{1,63} Q. Y. Zhang,^{40,81} Shuihan Zhang,^{1,63} Shulei Zhang,^{26,h} X. D. Zhang,⁴⁶ X. M. Zhang,¹ X. Y. Zhang,⁵⁰ Xuyan Zhang,⁵⁵ Y. Zhang,⁷² Y. Zhang,⁶⁹ Y. T. Zhang,⁸¹ Y. H. Zhang,^{1,58} Yan Zhang,^{71,58} Yao Zhang,¹ Z. H. Zhang,¹ Z. L. Zhang,³⁵ Z. Y. Zhang,⁷⁶ Z. Y. Zhang,⁴⁴ G. Zhao,¹ J. Zhao,⁴⁰ J. Y. Zhao,^{1,63} J. Z. Zhao,^{1,58} Lei Zhao,^{71,58} Ling Zhao,¹ M. G. Zhao,⁴⁴ S. J. Zhao,⁸¹ Y. B. Zhao,^{1,58} Y. X. Zhao,^{32,63} Z. G. Zhao,^{71,58} A. Zhemchugov,^{37,a} B. Zheng,⁷² J. P. Zheng,^{1,58} W. J. Zheng,^{1,63} Y. H. Zheng,⁶³ B. Zhong,⁴² X. Zhong,⁵⁹ H. Zhou,⁵⁰ L. P. Zhou,^{1,63} X. Zhou,⁷⁶ X. K. Zhou,⁷ X. R. Zhou,^{71,58} X. Y. Zhou,⁴⁰ Y. Z. Zhou,^{13,f} J. Zhu,⁴⁴ K. Zhu,¹ K. J. Zhu,^{1,58,63} L. Zhu,³⁵ L. X. Zhu,⁶³ S. H. Zhu,⁷⁰ S. Q. Zhu,⁴³ T. J. Zhu,^{13,f} W. J. Zhu,^{13,f} Y. C. Zhu,^{71,58} Z. A. Zhu,^{1,63} J. H. Zou,¹ and J. Zu^{71,58}

(BESIII Collaboration)

¹Institute of High Energy Physics, Beijing 100049, People's Republic of China

²Beihang University, Beijing 100191, People's Republic of China

³Beijing Institute of Petrochemical Technology, Beijing 102617, People's Republic of China

⁴Bochum Ruhr-University, D-44780 Bochum, Germany

- ⁵*Budker Institute of Nuclear Physics SB RAS (BINP), Novosibirsk 630090, Russia*
- ⁶*Carnegie Mellon University, Pittsburgh, Pennsylvania 15213, USA*
- ⁷*Central China Normal University, Wuhan 430079, People's Republic of China*
- ⁸*Central South University, Changsha 410083, People's Republic of China*
- ⁹*China Center of Advanced Science and Technology, Beijing 100190, People's Republic of China*
- ¹⁰*China University of Geosciences, Wuhan 430074, People's Republic of China*
- ¹¹*Chung-Ang University, Seoul 06974, Republic of Korea*
- ¹²*COMSATS University Islamabad, Lahore Campus, Defence Road, Off Raiwind Road, 54000 Lahore, Pakistan*
- ¹³*Fudan University, Shanghai 200433, People's Republic of China*
- ¹⁴*GSI Helmholtzcentre for Heavy Ion Research GmbH, D-64291 Darmstadt, Germany*
- ¹⁵*Guangxi Normal University, Guilin 541004, People's Republic of China*
- ¹⁶*Guangxi University, Nanning 530004, People's Republic of China*
- ¹⁷*Hangzhou Normal University, Hangzhou 310036, People's Republic of China*
- ¹⁸*Hebei University, Baoding 071002, People's Republic of China*
- ¹⁹*Helmholtz Institute Mainz, Staudinger Weg 18, D-55099 Mainz, Germany*
- ²⁰*Henan Normal University, Xinxiang 453007, People's Republic of China*
- ²¹*Henan University, Kaifeng 475004, People's Republic of China*
- ²²*Henan University of Science and Technology, Luoyang 471003, People's Republic of China*
- ²³*Henan University of Technology, Zhengzhou 450001, People's Republic of China*
- ²⁴*Huangshan College, Huangshan 245000, People's Republic of China*
- ²⁵*Hunan Normal University, Changsha 410081, People's Republic of China*
- ²⁶*Hunan University, Changsha 410082, People's Republic of China*
- ²⁷*Indian Institute of Technology Madras, Chennai 600036, India*
- ²⁸*Indiana University, Bloomington, Indiana 47405, USA*
- ^{29a}*INFN Laboratori Nazionali di Frascati, INFN Laboratori Nazionali di Frascati, I-00044 Frascati, Italy*
- ^{29b}*INFN Sezione di Perugia, I-06100 Perugia, Italy*
- ^{29c}*University of Perugia, I-06100 Perugia, Italy*
- ^{30a}*INFN Sezione di Ferrara, INFN Sezione di Ferrara, I-44122 Ferrara, Italy*
- ^{30b}*University of Ferrara, I-44122 Ferrara, Italy*
- ³¹*Inner Mongolia University, Hohhot 010021, People's Republic of China*
- ³²*Institute of Modern Physics, Lanzhou 730000, People's Republic of China*
- ³³*Institute of Physics and Technology, Peace Avenue 54B, Ulaanbaatar 13330, Mongolia*
- ³⁴*Instituto de Alta Investigación, Universidad de Tarapacá, Casilla 7D, Arica 1000000, Chile*
- ³⁵*Jilin University, Changchun 130012, People's Republic of China*
- ³⁶*Johannes Gutenberg University of Mainz, Johann-Joachim-Becher-Weg 45, D-55099 Mainz, Germany*
- ³⁷*Joint Institute for Nuclear Research, 141980 Dubna, Moscow region, Russia*
- ³⁸*Justus-Liebig-Universitaet Giessen, II. Physikalisches Institut, Heinrich-Buff-Ring 16, D-35392 Giessen, Germany*
- ³⁹*Lanzhou University, Lanzhou 730000, People's Republic of China*
- ⁴⁰*Liaoning Normal University, Dalian 116029, People's Republic of China*
- ⁴¹*Liaoning University, Shenyang 110036, People's Republic of China*
- ⁴²*Nanjing Normal University, Nanjing 210023, People's Republic of China*
- ⁴³*Nanjing University, Nanjing 210093, People's Republic of China*
- ⁴⁴*Nankai University, Tianjin 300071, People's Republic of China*
- ⁴⁵*National Centre for Nuclear Research, Warsaw 02-093, Poland*
- ⁴⁶*North China Electric Power University, Beijing 102206, People's Republic of China*
- ⁴⁷*Peking University, Beijing 100871, People's Republic of China*
- ⁴⁸*Qufu Normal University, Qufu 273165, People's Republic of China*
- ⁴⁹*Shandong Normal University, Jinan 250014, People's Republic of China*
- ⁵⁰*Shandong University, Jinan 250100, People's Republic of China*
- ⁵¹*Shanghai Jiao Tong University, Shanghai 200240, People's Republic of China*
- ⁵²*Shanxi Normal University, Linfen 041004, People's Republic of China*
- ⁵³*Shanxi University, Taiyuan 030006, People's Republic of China*
- ⁵⁴*Sichuan University, Chengdu 610064, People's Republic of China*
- ⁵⁵*Soochow University, Suzhou 215006, People's Republic of China*
- ⁵⁶*South China Normal University, Guangzhou 510006, People's Republic of China*
- ⁵⁷*Southeast University, Nanjing 211100, People's Republic of China*
- ⁵⁸*State Key Laboratory of Particle Detection and Electronics, Beijing 100049, Hefei 230026, People's Republic of China*
- ⁵⁹*Sun Yat-Sen University, Guangzhou 510275, People's Republic of China*
- ⁶⁰*Suranaree University of Technology, University Avenue 111, Nakhon Ratchasima 30000, Thailand*
- ⁶¹*Tsinghua University, Beijing 100084, People's Republic of China*

- ^{62a}*Turkish Accelerator Center Particle Factory Group, Istinye University, 34010, Istanbul, Turkey*
^{62b}*Near East University, Nicosia, North Cyprus, 99138, Mersin 10, Turkey*
⁶³*University of Chinese Academy of Sciences, Beijing 100049, People's Republic of China*
⁶⁴*University of Groningen, NL-9747 AA Groningen, The Netherlands*
⁶⁵*University of Hawaii, Honolulu, Hawaii 96822, USA*
⁶⁶*University of Jinan, Jinan 250022, People's Republic of China*
⁶⁷*University of Manchester, Oxford Road, Manchester M13 9PL, United Kingdom*
⁶⁸*University of Muenster, Wilhelm-Klemm-Strasse 9, 48149 Muenster, Germany*
⁶⁹*University of Oxford, Keble Road, Oxford OX13RH, United Kingdom*
⁷⁰*University of Science and Technology Liaoning, Anshan 114051, People's Republic of China*
⁷¹*University of Science and Technology of China, Hefei 230026, People's Republic of China*
⁷²*University of South China, Hengyang 421001, People's Republic of China*
⁷³*University of the Punjab, Lahore-54590, Pakistan*
^{74a}*University of Turin and INFN, University of Turin, I-10125 Turin, Italy*
^{74b}*University of Eastern Piedmont, I-15121 Alessandria, Italy*
^{74c}*INFN, I-10125, Turin, Italy*
⁷⁵*Uppsala University, Box 516, SE-75120 Uppsala, Sweden*
⁷⁶*Wuhan University, Wuhan 430072, People's Republic of China*
⁷⁷*Xinyang Normal University, Xinyang 464000, People's Republic of China*
⁷⁸*Yantai University, Yantai 264005, People's Republic of China*
⁷⁹*Yunnan University, Kunming 650500, People's Republic of China*
⁸⁰*Zhejiang University, Hangzhou 310027, People's Republic of China*
⁸¹*Zhengzhou University, Zhengzhou 450001, People's Republic of China*

^aAlso at the Moscow Institute of Physics and Technology, Moscow 141700, Russia.

^bAlso at the Novosibirsk State University, Novosibirsk 630090, Russia.

^cAlso at the NRC "Kurchatov Institute," PNPI, 188300 Gatchina, Russia.

^dAlso at Goethe University Frankfurt, 60323 Frankfurt am Main, Germany.

^eAlso at Key Laboratory for Particle Physics, Astrophysics and Cosmology, Ministry of Education; Shanghai Key Laboratory for Particle Physics and Cosmology; Institute of Nuclear and Particle Physics, Shanghai 200240, People's Republic of China.

^fAlso at Key Laboratory of Nuclear Physics and Ion-beam Application (MOE) and Institute of Modern Physics, Fudan University, Shanghai 200443, People's Republic of China.

^gAlso at State Key Laboratory of Nuclear Physics and Technology, Peking University, Beijing 100871, People's Republic of China.

^hAlso at School of Physics and Electronics, Hunan University, Changsha 410082, China.

ⁱAlso at Guangdong Provincial Key Laboratory of Nuclear Science, Institute of Quantum Matter, South China Normal University, Guangzhou 510006, China.

^jAlso at Frontiers Science Center for Rare Isotopes, Lanzhou University, Lanzhou 730000, People's Republic of China.

^kAlso at Lanzhou Center for Theoretical Physics, Lanzhou University, Lanzhou 730000, People's Republic of China.

^lAlso at the Department of Mathematical Sciences, IBA, Karachi 75270, Pakistan.